Catalysis Letters 29 (1994) 77–90

Local structure determination of aluminum in Y zeolite: application of low energy X-ray absorption fine structure spectroscopy

D.C. Koningsberger [a,1] and J.T. Miller [b]

[a] *Laboratory of Inorganic Chemistry and Catalysis, Debye Institute, Utrecht University, PO Box 80083, 3508 TB Utrecht, The Netherlands*

[b] *Amoco Research Center, 150 W. Warrenville Rd., Naperville, IL 60566-7011, USA*

Received 20 July 1994; accepted 8 August 1994

The local Al structure and electronic properties in Na-Y, NH_4-Y and H-Y zeolites have been determined by low energy Al XAFS. The Al–O bond distance of 1.700 Å in H-Y is longer than that in NH_4-Y and Na-Y, 1.636 and 1.620 Å, respectively. In addition, the white line intensity of the Al ion in H-Y is higher than in NH_4-Y and Na-Y, indicating the electron density on the Al ion is lower in H-Y than in the other two catalysts. The results of experimental Al–O bond distance and white line intensities are qualitatively in agreement with theoretically calculated Al–O bond distances in aluminosilicate clusters. However, further work is required in order to quantitatively evaluate the near edge structure of the X-ray absorption data.

Keywords: Al EXAFS; Al XAFS in Na-Y, NH_4-Y and H-Y; acidity; white line

1. Introduction

Solid acid catalysts play a prominent role in the development of catalytic processes in petrochemical industries. Current industrial processes are dominated by zeolite catalysts and include fluid catalytic cracking (FCC), hydrocracking, paraffin isomerization, aromatic alkylation, xylene isomerization, catalytic dewaxing, methanol-to-gasoline, etc. [1]. Of the industrial processes, FCC is by far the largest application of acidic zeolites accounting for approximately 20% of all catalyst sales [2]. Current FCC catalysts are based on modified Y zeolites [3]. The development of new and improved zeolite catalysts depends on a better understanding of the relationship between acidity and catalytic performance.

The structure of zeolites is composed of oxide tetrahedra of silicon and aluminum. Charge balance requires that for each aluminum there is one cation [1]. It is generally accepted that in acidic zeolites the active site is a Brønsted acid localized

[1] To whom correspondence should be addressed.

on an oxygen ion of the aluminum tetrahedra [4,5]. The strength of the Brønsted acid is affected by several factors, such as the presence of alkali [6,7] and other cations [8,9], the silicon-to-aluminum ratio [10,11], the presence of extra-framework aluminum [12–16], the structure of the zeolite, etc. [17].

Numerous experimental techniques have been applied for determination of the number, strength and type of acid sites. The number of sites may be determined by adsorption of a base, e.g., propyl-ammine, which adsorbs in a one-to-one complex on acid sites [18]. Although this technique allows for the determination of the number of acid sites, it is not possible to determine the strength of the acid sites. The number and average acid strength can be determined by temperature programmed desorption of ammonia [19,20]. For many zeolites of interest, however, physisorbed and chemisorbed ammonia desorb at overlapping temperatures leading to inaccurate determination of both the number and strength of acid sites. Infrared spectroscopy of adsorbed pyridine has been widely used to identify the number of Brønsted and Lewis acid sites in zeolites [21,22].

In addition to adsorption of bases, the number of acid sites can be determined spectroscopically. For example, in Y zeolite X-ray diffraction (XRD) can be used to determine the number of aluminums in the zeolite lattice [23–25]. Structural analysis of zeolites by XRD, however, does not provide information about the local Al–O distance since most lattice sites are occupied by silicon. Al NMR can be used to determine the oxygen coordination of the Al ions. Tetrahedral (structural) aluminum ions have an Al resonance at 55 ppm, while a resonance at 0 ppm indicates octahedral (non-structural) aluminum ions [26,27].

It is expected that the local structural properties of the aluminum tetrahedron sites determine the catalytic properties of this Brønsted acid site. Al–O distances can be studied by neutron powder diffraction using Rietveld analysis [28]. From the numerous techniques which have been applied for the characterization of zeolites, the only technique which allows for a direct determination of the Al–O distance or the charge on the Al ion is X-ray absorption fine structure spectroscopy. XAFS spectroscopy has been used to study the change of the local structure of Al in zeolite Y after the incorporation of nickel ions [29].

The purpose of this paper is to demonstrate the sensitivity of low energy X-ray absorption spectroscopy for changes in the local structure around the Al ion in zeolite Y as a function of the zeolite acidity. In addition, the changes in the Al–O coordination environment in Na-Y, NH_4-Y and H-Y are compared with predictions from theoretical calculations.

2. Experimental

Na-Y was a commercial zeolite (LZY-54) purchased from UOP. The sample crystallinity was confirmed by SEM and XRD and had a unit cell dimension of 24.676 Å, ca. 56 Al/unit cell. Al NMR confirmed all of the Al was in tetrahedral

coordination. NH_4-Y was prepared by repeated ammonium exchange. 150 g of Na-Y was exchanged with 10 × 1 ℓ of 2 M NH_4NO_3 at 80°C for 3 h. Following the final exchange the zeolite was washed with 3 × 1 ℓ 80°C H_2O for 1 h and dried at 125°C. The elemental Na analysis was 0.13 wt%. SEM confirmed the NH_4-Y was highly crystalline. The XRD unit cell parameter had expanded to 24.729 Å and Al NMR confirmed that all the Al was in tetrahedral coordination. H-Y was prepared by careful calcination of NH_4-Y. NH_4-Y was dried at 125°C overnight. The temperature was raised to 200°C for 3 h, 250°C for 3 h and finally to 300°C for 3 h. The crystallinity by XRD was 98% based on Na-Y as a standard and the unit cell dimension was 24.643 Å, or 52 Al/unit cell. Al NMR indicated that 85% of the Al were in tetrahedral coordination with 15% in octahedral coordination.

EXAFS measurements of the catalysts were performed at the soft X-ray XAFS station 3.4 of the SRS at Daresbury (UK). This station is operating with a double quartz crystal monochromator. Harmonic contamination of the X-ray beam is small due to the use of collimating mirrors. The estimated resolution was 1.5 eV at the Al K-edge (1559 eV). The data were collected simultaneously with a fluorescence and an electron yield detector. Datum was collected with *k*-space scan mode (start, 3 s; end, 30 s). Six scans were averaged in order to minimize both high and low frequency noise.

The samples were mixed with carbon and mounted with epoxy onto the face of the stainless steal sample holder. No signal from the epoxy or the sample holder could be detected. XAFS measurements were conducted under vacuum (typically 10^{-7} Torr) at room temperature. Electron yield spectra indicate no distortion of the X-ray absorption coefficient, while fluorescence spectra are reduced in amplitude due to absorption by the sample [30]. As a result, the near edge spectra were determined from the electron yield spectra. The instrumental background signal of the electron yield channel prevented a reliable determination of the EXAFS background at high *k* values. Therefore, the fluorescence data were used to generate the EXAFS function. Standard procedures were used to extract the EXAFS spectrum from the experimental absorption spectrum. Normalization was done by dividing by the height of the absorption edge and the background was subtracted using cubic spline routines [31,32]. The errors in the structural parameters were calculated from the covariance matrix taking into account the statistical noise of the EXAFS data and the correlations between the different coordination parameters [33]. The average statistical deviation in the noise amplitude in the raw data was calculated from the average of the six scans and was 0.003. The values of the goodness of fit (ε_ν^2) were calculated as outlined in the Reports on Standard and Criteria in XAFS Spectroscopy [34].

Reference phase shifts and back-scattering amplitude functions of the Al–O absorber back-scatter pair were determined for $AlPO_4$ (tetrahedral Al–O) both in electron yield and fluorescence mode. The purity of the aluminum phosphate ($AlPO_4$) EXAFS standard was confirmed by XRD and Al NMR.

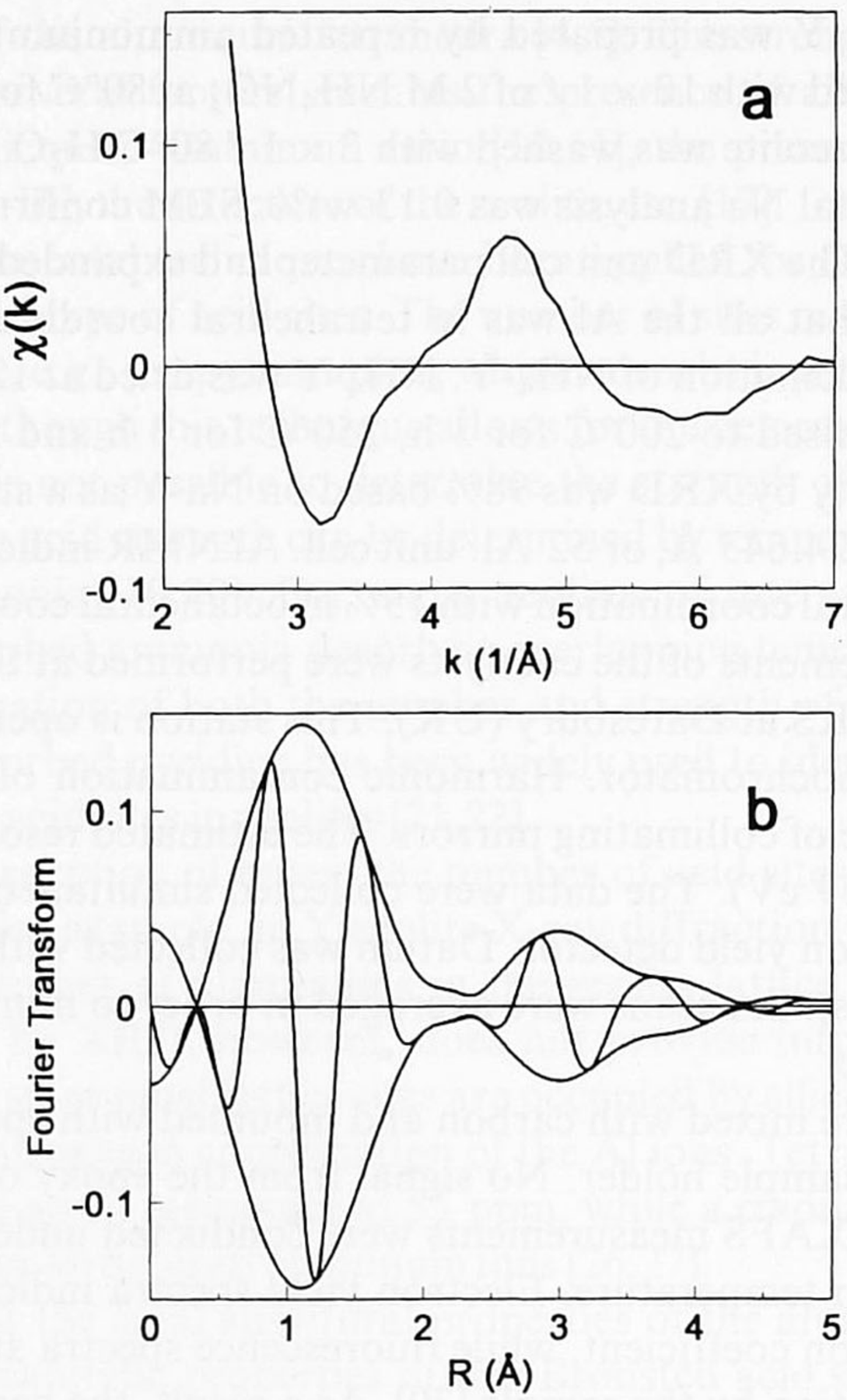

Fig. 1. (a) EXAFS data (average of six scans) of $AlPO_4$, (b) Fourier transform (k^1, $\Delta k = 2.8$–7.1 $Å^{-1}$) of the EXAFS data.

3. Results

3.1. REFERENCE COMPOUND

The averaged raw EXAFS data of the Al–O reference $AlPO_4$ is shown in fig. 1a, and the corresponding Fourier transform is presented in fig. 1b. The determination of the reference functions is straightforward, since the first shell Al–O distance in r space shows no overlap with higher shells. The crystallographic first shell coordination parameters for the reference compound, the weighting of the Fourier transform, the ranges in k and r space used to extract the reference functions from the experimental EXAFS data are given in table 1. Due to the Fourier

Table 1
Crystallographic data and Fourier filtering ranges of reference compounds

Compound	Ab–Sc pair	k^n	FT range ($Å^{-1}$)	Filter range (Å)	N	R (Å)
$AlPO_4$	Al–O	1	2.8–7.1	0.3–2.3	4	1.73

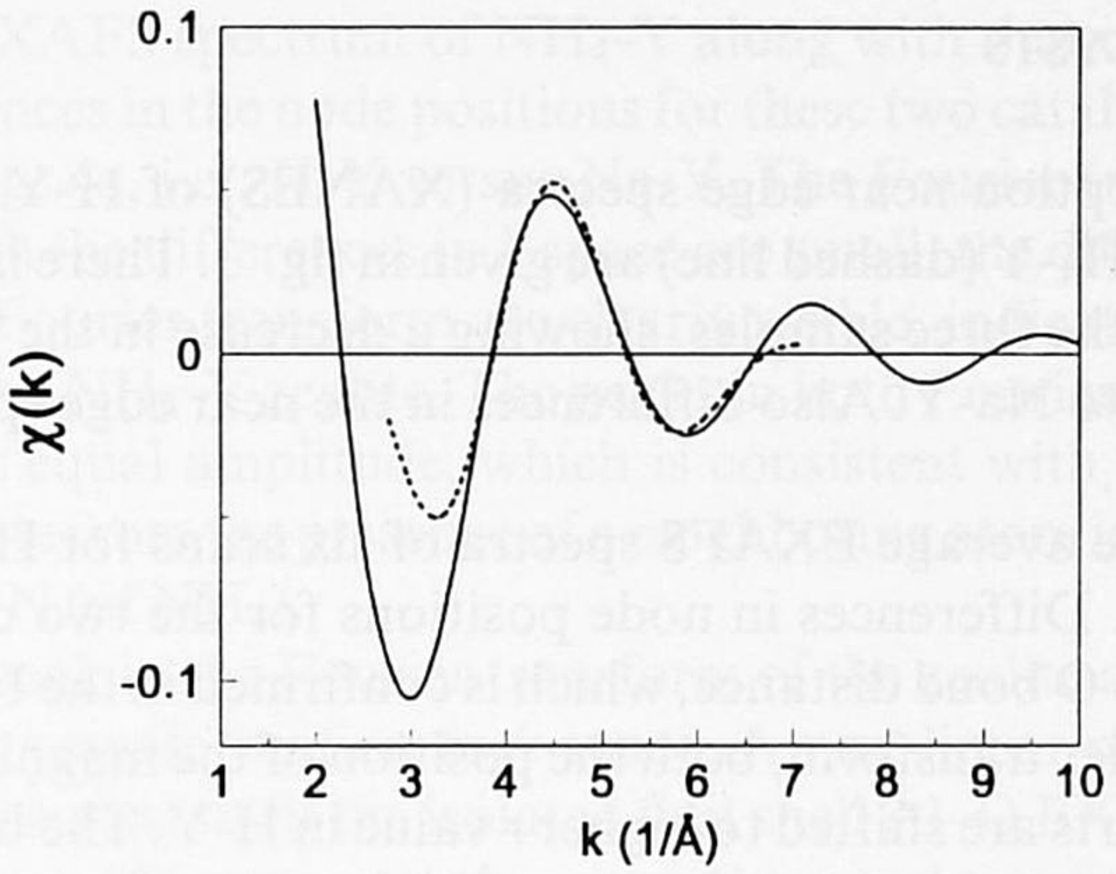

Fig. 2. Extended theoretical EXAFS reference function (solid line) and isolated first shell EXAFS obtained from $AlPO_4$ (dotted line), for details see text and table 1.

filtering, the obtained phase shifts and back scattering amplitudes are only reliable from $3.5 < k < 6.5$ Å^{-1}. In order to analyze the EXAFS data over a wider k range, the Fourier filtered first shell experimental data of the $AlPO_4$ reference was extended at low and high k by fitting the data using a theoretically calculated phase shift and back scattering amplitude obtained from FEFF 3.1. The input parameters for the calculation were $N = 4$, $R = 1.70$ Å, $S_0^2 = 0.8$ and $\sigma^2 = 0.000$. The extended EXAFS reference function and the isolated first shell experimental data are shown in fig. 2.

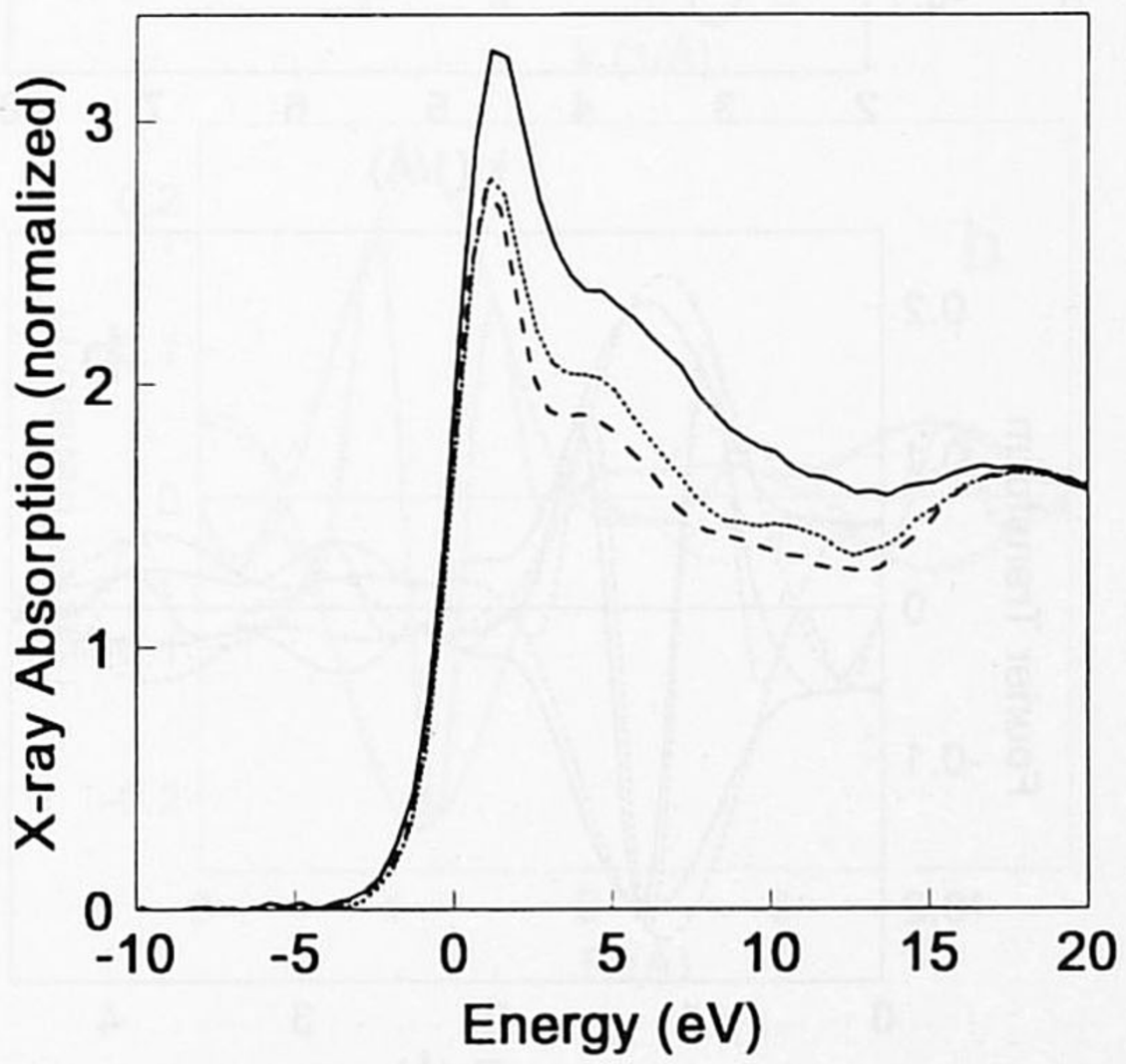

Fig. 3. X-ray absorption near edge spectra of H-Y (solid line), NH_4-Y (dotted line) and Na-Y (dashed line).

3.2. ZEOLITE CATALYSTS

The X-ray absorption near edge spectra (XANES) of H-Y (solid line), Na-Y (dotted line) and NH_4-Y (dashed line) are given in fig. 3. There is a clear distinction in the white line of the three samples, showing a decrease in the white line intensity in going from H-Y to Na-Y. Also differences in the near edge spectra are observed around 5 and 12 eV.

Fig. 4a shows the average EXAFS spectra of six scans for H-Y (solid line) and Na-Y (dotted line). Differences in node positions for the two catalysts indicate a difference in the Al–O bond distance, which is confirmed in the Fourier transforms, fig. 4b. In the Fourier transform, both the position of the magnitude and the nodes of the imaginary parts are shifted to higher r value in H-Y. The high signal-to-noise ratio of the data allows for the detection of higher coordination shells. The peak around 3.8 Å in the Fourier transform of Na-Y is possibly caused by the presence of Na ions in the second coordination sphere of Al.

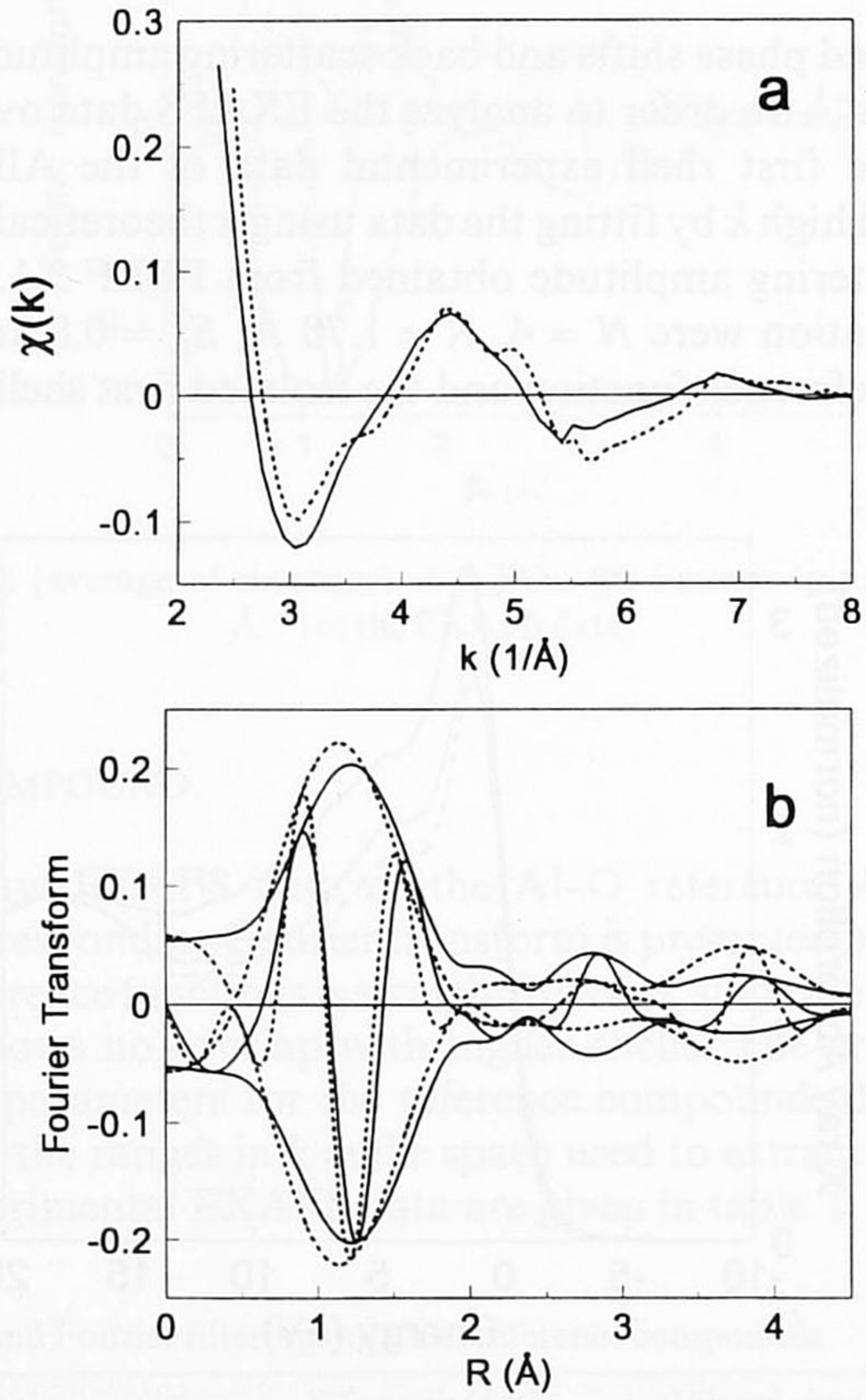

Fig. 4. (a) EXAFS data (average of six scans) of H-Y (solid line) and Na-Y (dotted line), (b) Fourier transform (k^1, $\Delta k = 2.7$–8.0 Å^{-1}) of the EXAFS data of H-Y (solid line) and Na-Y (dotted line).

The averaged EXAFS spectrum of NH_4-Y along with that of Na-Y is shown in fig. 5a. The differences in the node positions for these two catalysts are much smaller than those in fig. 4a, i.e., H-Y versus Na-Y. The Fourier transforms are given in fig. 5b. Although the differences in k space are small, the differences in the imaginary part of the Fourier transform are clearly visible, indicating a slightly larger Al–O distance in the NH_4-Y zeolite. The peaks in both Fourier transforms around 3.8 Å have almost equal amplitude, which is consistent with the suggestion that these peaks originate from the presence of a neighboring atom in the second coordination shell, Na or N (of NH_4).

The first Al–O peak in the Fourier transform of the zeolite samples are isolated by inverse Fourier transformation to k space. A non-linear multiple shell fitting routine [33] has been used to fit the isolated first shell Al–O EXAFS. The details of the fitting procedure (fit ranges in k space, the number of independent points

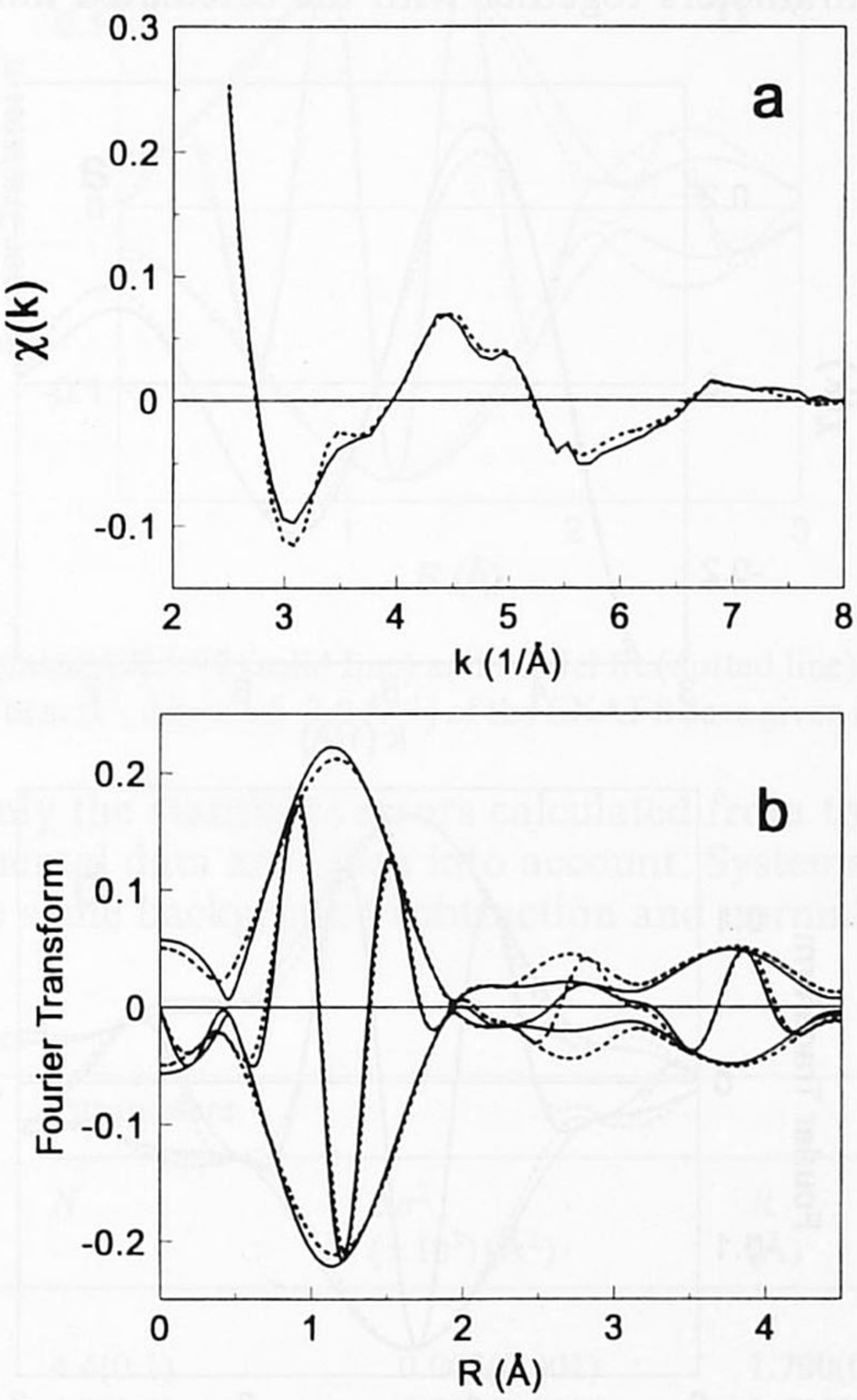

Fig. 5. (a) EXAFS data (average of six scans) of Na-Y (solid line) and NH_4-Y (dotted line), (b) Fourier transform ($k^1, \Delta k = 2.7$–8.0 Å^{-1}) of the EXAFS data of Na-Y (solid line) and NH_4-Y (dotted line).

Table 2
Fourier filter and analysis ranges. Values for N_{indp} [a], ν [b] and ε_ν^2 [c]

Sample	FT weight k^n	FT range (Å^{-1})	Filter range (Å)	Fit weight k^n	Analysis range (Å^{-1})	N_{indp}	ν	Max. noise amplitude	ε_ν^2
H-Y	2	2.6–8.1	0.4–2.3	1	3.2–7.5	6.9	2.9	0.003	5
NH_4-Y	2	2.7–8.1	0.3–2.2	1	3.5–7.0	5.2	1.2	0.003	15
Na-Y	2	2.7–7.9	0.3–2.1	1	3.5–7.0	5.0	1.0	0.003	19

[a] N_{indp} is number of independent parameters; $N_{indp} = 2\Delta k \Delta R/\pi + 1$.
[b] ν is degree of freedom; $\nu = N_{indp} - N_{fit}$.
[c] ε_ν^2, see ref. [34].

(N_{indp}), the degrees of freedom (N_{free}), and the goodness of fit values (ε_ν^2)) are given in table 2. The first shell isolated EXAFS and Fourier transform and the model fits are given in figs. 6, 7 and 8 for H-Y, NH_4-Y and Na-Y, respectively. The resulting coordination parameters together with the calculated limits of accuracy are

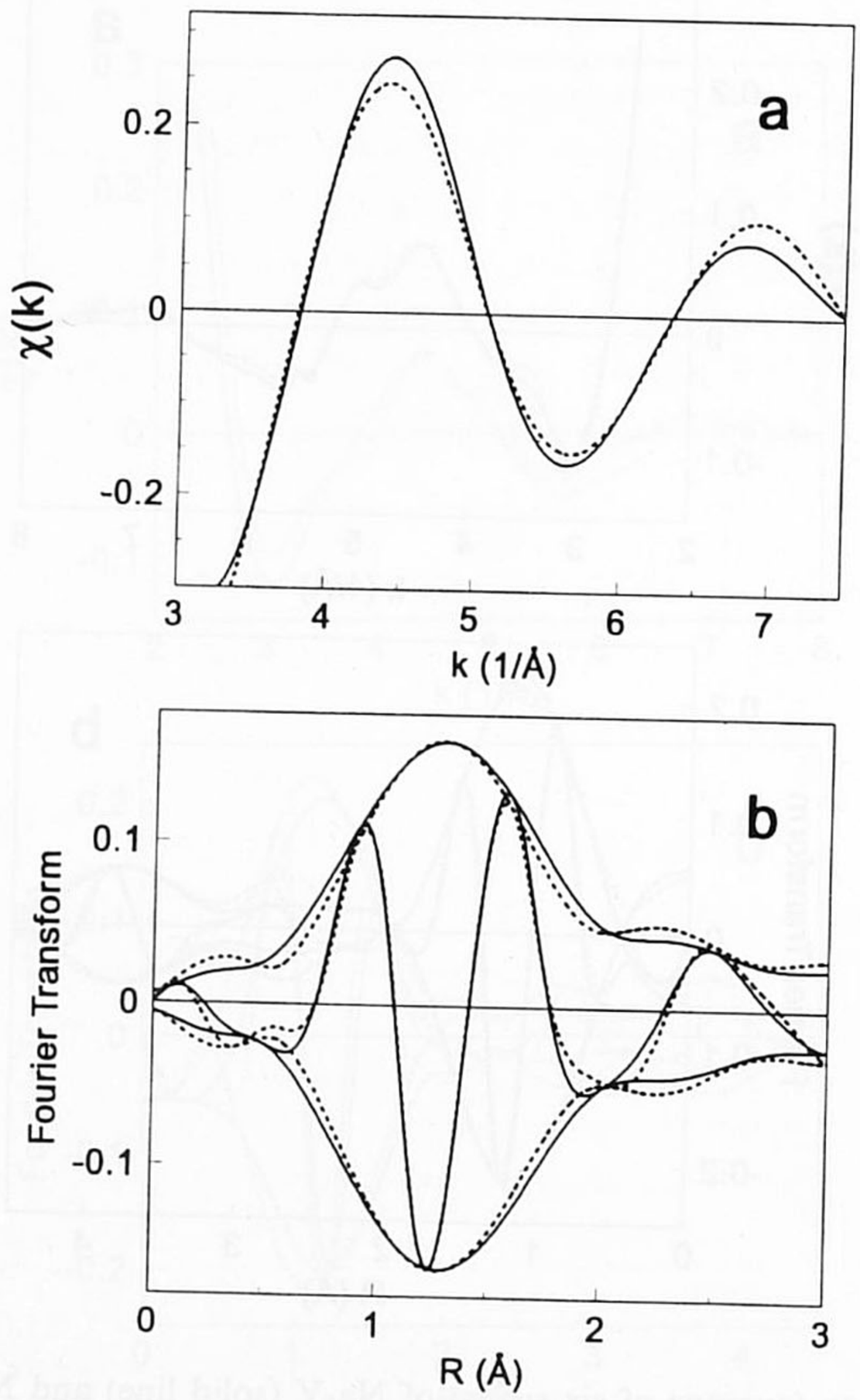

Fig. 6. (a) First shell isolated EXAFS (solid line) and model fit (dotted line) of H-Y, (b) Fourier transform (k^1, $\Delta k = 3.2$–7.5 Å^{-1}) of the EXAFS data given in (a).

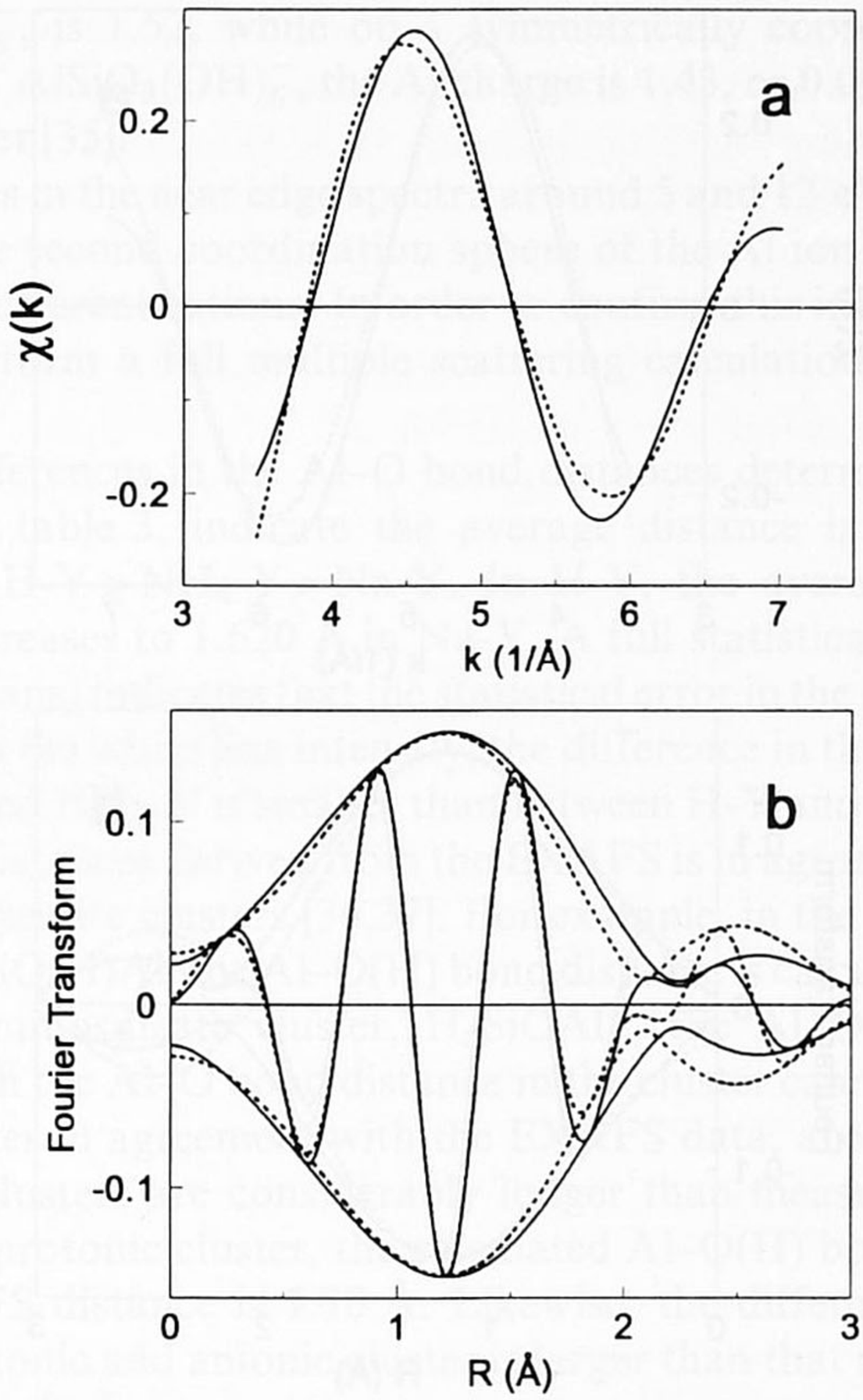

Fig. 7. (a) First shell isolated EXAFS (solid line) and model fit (dotted line) of NH_4-Y, (b) Fourier transform (k^1, $\Delta k = 3.5$–7.0 Å^{-1}) of the EXAFS data given in (a).

given in table 3. Only the statistical errors calculated from the averaging procedure of the experimental data are taken into account. Systematic errors are minimized by using the same background subtraction and normalization procedures

Table 3
Coordination parameters [a]

	Parameters			
	N	$\Delta\sigma^2$ ($\times 10^3$) (Å^2)	R (Å)	ΔE_0 (eV)
coordination: Al–O				
H-Y	4.4(0.1)	0.003(0.001)	1.700(0.003)	2.0(0.4)
NH_4-Y	4.2(0.1)	0.003(0.001)	1.636(0.003)	7.5(0.2)
Na-Y	3.8(0.1)	−0.005(0.001)	1.620(0.003)	8.6(0.3)

[a] Numbers between parentheses are limits of accuracy as calculated from a full statistical analysis of the data including the standard deviation per data point (see text).

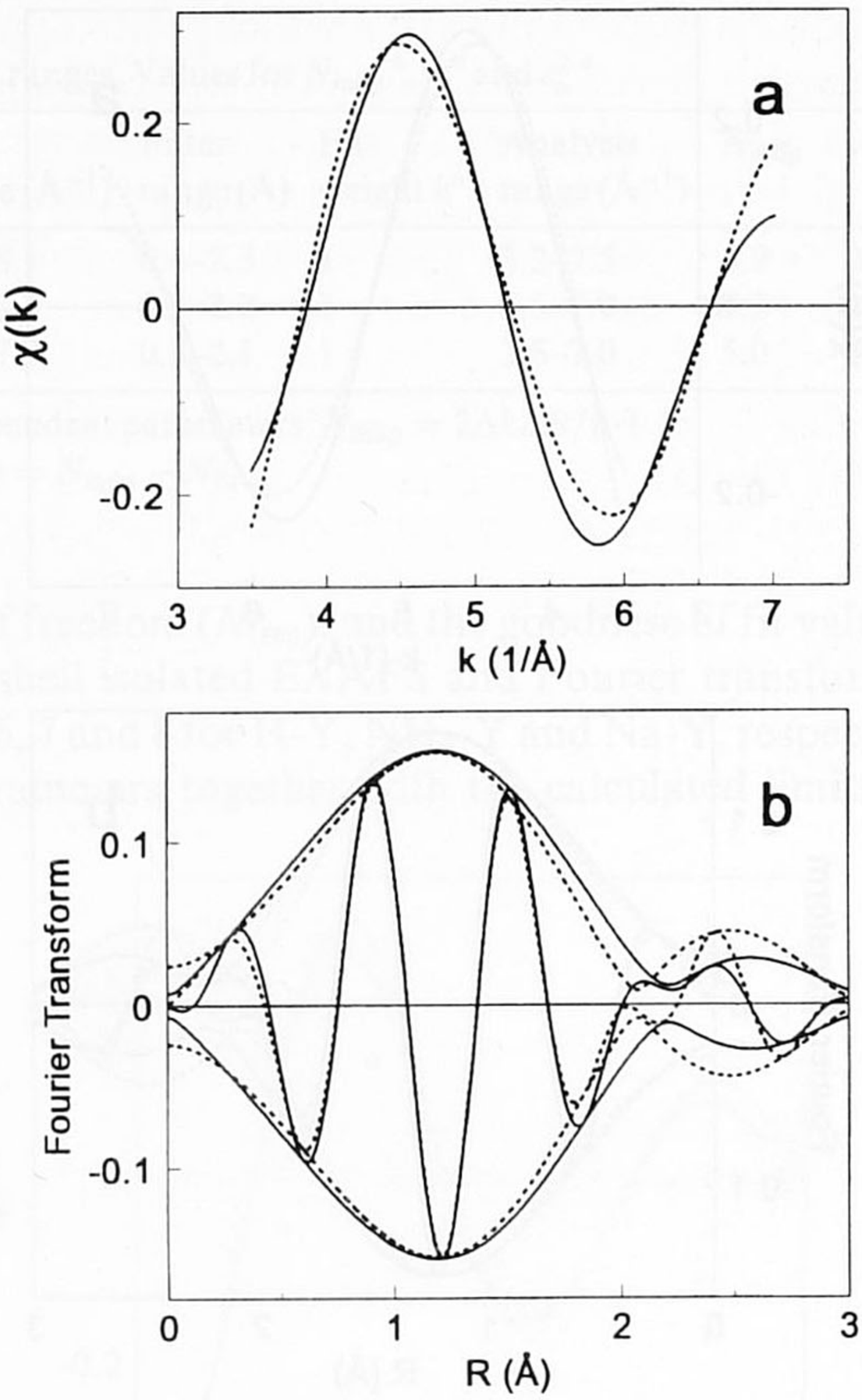

Fig. 8. (a) First shell isolated EXAFS (solid line) and model fit (dotted line) of Na-Y, (b) Fourier transform (k^1, $\Delta k = 3.5$–7.0 Å^{-1}) of the EXAFS data given in (a).

for all data sets and by careful calibration of the reference phase shift and back-scattering amplitudes.

4. Discussion

As shown in fig. 3 the white line intensity, representing a 1s to 3p transition, is sensitive to the composition of the zeolite. The white line intensity is highest for H-Y and decreases in the order H-Y > NH_4-Y > Na-Y. The differences in the white line intensity between NH_4-Y and Na-Y are much smaller than the differences between H-Y and NH_4-Y. The highest white line intensity in H-Y indicates the electron density on the Al is lowest in H-Y and increases in the order H-Y > NH_4-Y > Na-Y. The order of the electron densities derived from the white line intensities is in agreement with theoretical calculations for zeolite clusters. For example, the positive charge on Al for a protonated aluminosilicate ring,

$H^+ AlSiO_3(OH)_6^-$, is 1.52, while on a symmetrically coordinated Na-aluminosilicate ring, $Na^+ AlSiO_3(OH)_6^-$, the Al charge is 1.43, or 0.09 electrons less on the protonated cluster [35].

The differences in the near edge spectra around 5 and 12 eV appear to be related to changes in the second coordination sphere of the Al ion corresponding to the presence of the different cations. In order to confirm this interpretation, it will be necessary to perform a full multiple scattering calculation of the Al near edge spectra.

Structural differences in the Al–O bond distances determined from the fitting of the EXAFS, table 3, indicate the average distance is largest in H-Y and decreases from H-Y > NH_4-Y > Na-Y. In H-Y, the average Al–O distance is 1.700 Å and decreases to 1.620 Å in Na-Y. A full statistical analysis of the data (average of six scans) indicates that the statistical error in the Al–O bond distance is 0.003 Å. As with the white line intensity, the difference in the Al–O bond distance between Na-Y and NH_4-Y is smaller than between H-Y and NH_4-Y. The order of the Al–O bond distances derived from the EXAFS is in agreement with theoretical calculations for zeolite clusters [36,37]. For example, in the protonic aluminosilicate cluster, $H_6SiO(H)Al$, the Al–O(H) bond distance is calculated to be 2.03 Å. In the anionic aluminosilicate cluster, H_6SiOAl^-, the Al–O bond is reduced to 1.79 Å. Although the Al–O bond distance in the cluster calculations is smaller for the anionic cluster in agreement with the EXAFS data, absolute Al–O bond distances in both clusters are considerably longer than measured by EXAFS. For example, in the protonic cluster, the calculated Al–O(H) bond distance is 2.03 Å while the EXAFS distance is 1.70 Å. Likewise, the difference in bond distance between the protonic and anionic cluster is larger than that measured by EXAFS, e.g., 0.24 versus 0.08 Å.

EXAFS, however, measures the (time) average of all the Al–O bond distances. In the cluster calculations, the remaining three Al–O bond distances are 1.57 Å in the protonic cluster and 1.60 Å in the anionic cluster. The average of the distances obtained from the theoretical calculations is, therefore, 1.69 Å for the protonic cluster and 1.65 Å for the anionic cluster, in excellent agreement with the EXAFS determinations of 1.700 Å for H-Y and 1.620 Å for Na-Y.

The original cluster calculations of the NH_4^+ H_6SiOAl^- cluster predicted that the Al–O bond distance was identical to that of the protonic cluster [36]. The model assumed a weak interaction between the ammonia and the proton. However, when hydrogen bonding between the ammonium ion and the oxide lattice is taken into account, the calculations predict a structure similar to that of the anionic (Na) cluster with an Al–O distance of 1.79 Å [37]. Comparison of the EXAFS Al–O bond distance in NH_4-Y with H-Y and Na-Y indicates that the NH_4-Y is more nearly similar to Na-Y than H-Y. The EXAFS data for NH_4-Y is consistent with the theoretical model where the ammonium ion is hydrogen bonded to the oxide lattice.

The local structural determination of the Al environment in Y zeolite with different cations by low energy Al EXAFS is in agreement with the theoretical calcula-

tions carried out on different model clusters. From the cluster calculations, as the electron densities of the Al ions decrease with changing cation, i.e., increasing positive charge, the white line intensity increases. In addition, the changes in the Al–O bond distance determined by EXAFS as a function of the cation type are in agreement with the values obtained from the cluster calculations. Both the white line and the Al–O bond distance determined from the experimental data indicate that the theoretical calculations of the clusters contain the essential information about the local structure and electronic properties of Al in the zeolite catalysts. This suggests that the cluster calculations can be used to quantitatively evaluate the XANES spectra, including the features at 5 and 12 eV.

Comparison of the XANES and EXAFS for H-Y and Na-Y indicates that Al X-ray absorption spectroscopy may be used as a scale for zeolite acidity. For example, the white line was much larger in H-Y than in Na-Y. If the charge on the Al ion affects the acidity of the hydroxyl, then quantitative analysis of the white line should be a sensitive measure of the acid strength. As discussed above, this will require a more quantitative evaluation of the white line. In addition, accurate determination of the Al–O bond distance may also represent a scale of acidity. However, the differences in bond length from H-Y to Na-Y were 0.08 Å. These two zeolites represent a large difference in acidity from strongly acidic to non-acidic. Small changes in acid strength, therefore, which may be catalytically important may not be detected by the change in Al–O bond distance.

This study demonstrates the current capability for Al EXAFS data acquisition and analysis. Improvement of the data quality should be possible with the use of new, third generation synchrotrons and future development of low noise, low energy beam line components. With a fully optimized beam line, it may be possible to extend the data range in k space to 8.5 $Å^{-1}$ before the Si edge in zeolites overlaps with the data from the Al edge. Many of the zeolites contain much less Al than those of the current study. In order to obtain acceptable data quality, improved sensitivity in the detection limits is required. For many of the future problems, in situ fluorescence and electron yield cells will be required.

5. Conclusions

This paper demonstrates the application of low energy Al XAFS for the characterization of the local Al structure and electronic properties in zeolites. The results for the catalysts in this study indicate that Al XAFS is sensitive to the zeolite acidity. Continued development of the technique may lead to a sensitive method for evaluating the acidity of zeolite catalysts. The experimental results are in good agreement with theoretical calculations on aluminosilicate clusters. Further theoretical work is required in order to fully understand the near edge structure of the X-ray absorption data.

Acknowledgement

The authors would like to thank Jim Kaduc for the XRD evaluation of the $AlPO_4$ standard and determinations of crystallinity and unit cell determination and Joe Ray for obtaining the Al NMR spectra on the $AlPO_4$ and zeolite samples. The authors would also like to thank Roland Vogels, Barbara Mojet, Geert Kruizinga and Andrea Russell for assistance in collection of the EXAFS data. DCK would like to thank the NWO for financial support of this research.

References

[1] S. Bhatia, *Zeolite Catalysis: Principles and Applications* (CRC Press, Boca Raton, 1990).
[2] S.C. Stinson, Chem. Eng. News 61 (49) (1983) 19.
[3] J. Scherzer, *Octane-Enhancing Zeolitic FCC Catalysts: Scientific and Technical Aspects* (Dekker, New York, 1990).
[4] W.O. Haag, R.M. Lago and P.B. Weisz, Nature 309 (1984) 989.
[5] J.R. Sohn, S.J. De Canio, P.O. Fritz and J.H. Lunsford, J. Phys. Chem. 90 (1986) 4847.
[6] J.W. Ward, J. Catal. 13 (1969) 321.
[7] J.S. Magee and J.J. Blazek, in: *Zeolite Chemistry and Catalysis*, ACS Monograph 171, ed. J. Rabo (Am. Chem. Soc., Washington, 1976) p. 615.
[8] W.M. Meier and D.H. Olson, Adv. Chem. Ser. 102 (1971) 155.
[9] P.O. Fritz and J.H. Lunsford, J. Catal. 119 (1989) 85.
[10] D. Barthomeuf, in: *Catalysis 1987*, ed. J.W. Ward (Elsevier, Amsterdam, 1988) p. 177.
[11] H. Starch, J. Janchen and U. Lohse, Catal. Lett. 13 (1992) 389.
[12] C. Mirodatos, B.H. Ha, K. Otsuka and D. Barthomeuf, in: *Proc. 5th Int. Conf. on Zeolites*, Naples, ed. L.V.C. Rees (1980) p. 382.
[13] C. Mirodatos and D. Barthomeuf, J. Chem. Soc. Chem. Commun. (1981) 39.
[14] R.M. Lago, W.O. Haag, R.J. Mikovsky, D.H. Olson, S.D. Hellring, K.D. Schmitt and G.T. Kerr, in: *New Developments in Zeolite Science and Technology*, Proc. 7th Int. Zeolite Conf., Tokyo, eds. Y. Murakami, A. Lyima and J.W. Ward (1986) p. 677.
[15] R. Carvajal, P.-J Chu and J.H. Lunsford, J. Catal. 125 (1990) 123.
[16] R.A. Beyerlein, G.B. McVicker, L.N. Yacullo and L.N. Ziemiak, J. Phys. Chem. 92 (1988) 1967.
[17] R. Carson, E.M. Cooke, J. Dwyer, A. Hinchliffe and P.J. O'Malley, in: *Zeolites as Catalysts, Sorbents, and Detergent Builders: Applications and Innovations*, Proc. Int. Symp., Stud. Surf. Sci. Catal., Vol. 46, eds. H.G. Karge and J. Weitkamp (Elsevier, Amsterdam, 1989) p. 39.
[18] T.J.G. Kofke, R.J. Gorte and W.E. Farneth, J. Catal. 114 (1988) 34.
[19] J.G. Post and J.H.C. van Hooff, Zeolites 4 (1984) 9.
[20] M. Niwa, M. Iwamoto and K. Segawa, Bull. Chem. Soc. Jpn. (1986) 1735.
[21] J.E. Mapes and R.P. Eischens, J. Phys. Chem. 58 (1954) 1059.
[22] E.P. Parry, J. Catal. 2 (1963) 371.
[23] H. Fichtner-Schmittler, U. Lohse, G. Engelhardt and V. Patzelova, Cryst. Res. Techn. 19 (1984) K1.
[24] J.R. Sohn, J. DeCanio, J.H. Lunsford and D.J. O'Donnell, Zeolites 6 (1986) 225.
[25] G.T. Kerr, Zeolites 9 (1989) 350.
[26] J.M. Thomas and J. Klinowski, Adv. Catal. 33 (1985) 199.
[27] G. Engelhardt and D. Michel, *High Resolution Solid-State NMR of Silicates and Zeolites* (Wiley, New York, 1987) p. 150.

[28] A.K. Cheetham, J.T. Thomas, M.M. Eddy and D.A. Jefferson, Nature 299 (1982) 24.
[29] E. Dooryhee, G.N. Greaves, A.T. Steel, R.P. Townsend, S.W. Carr, J.M. Thomas and R.A. Catlow, Faraday Discussions Chem. Soc. 89 (1990) 119.
[30] S.M. Heald, in: *X-Ray Absorption: Principles, Applications, Techniques of EXAFS, SEXAFS and XANES*, eds. D.C. Koningsberger and R. Prins (Wiley, New York, 1988) p. 87.
[31] J.W. Cook Jr. and D.E. Sayers, J. Appl. Phys. 52 (1981) 5024.
[32] J.B.A.D. van Zon, D.C. Koningsberger, H.F. van't Blik and D.E. Sayers, J. Chem. Phys. 82 (1985) 5742.
[33] M. Vaarkamp, PhD Thesis, Eindhoven University of Technology, Eindhoven, The Netherlands (1993).
[34] F.W. Lyttle, D.E. Sayers, and E.A. Stern, Physica B 158 (1988) 701.
[35] R.A. van Santen, B.W.H. van Beest and A.J.M. de Man, in: *Guidelines for Mastering the Properties of Molecular Sieves*, ed. D. Barthomeuf et al. (Plenum Press, New York, 1990) p. 201.
[36] E.H. Teunissen, F.B. van Duijneveldt and R.A. van Santen, J. Phys. Chem. 96 (1992) 366.
[37] E.H. Teunissen, R.A. van Santen, A.P. Jansen and F.B. van Duijneveldt, J. Phys. Chem. 97 (1993) 203.